

Assessment of South Pars Gas Field Subsidence Due To Gas Withdrawal

Ghazifard, A.¹, Fatemi Aghda, S.M.² and Taherynia, M.H.^{3*}

¹ Associate Professor, Department of Geology, Faculty of Sciences, University of Isfahan, Isfahan, Iran.

² Associate Professor, Faculty of Erath Science, Kharazmi University, Tehran, Iran.

³ Ph.D. Student, Faculty of Erath Science, Kharazmi University, Tehran, Iran.

Received: 06 Jan. 2013;

Revised: 05 Oct. 2013;

Accepted: 06 Jan. 2014

ABSTRACT: Withdrawal of oil and gas from reservoirs causes a decrease in pore pressure and an increase in effective stress which results to a reservoir compaction. Reservoir compaction will result in surface subsidence through the elastic response of the subsurface. Usually in order to determine the subsidence above a hydrocarbon field, the reservoir compaction must be first calculated and then the effect of this compaction on the surface should be modeled. The use of the uniaxial compaction theory is more prevalent and an accepted method for determining the amount of reservoir compaction. But despite of the reservoir compaction calculation method, there are many methods with different advantages and shortcomings for modeling of surface subsidence. In this study, a simple analytical method and semi-analytical methods (Aesub software) were used for modeling of the surface subsidence of the South Pars gas field at the end of the production period.

Keywords: Compressibility, Influence Function, Reservoir Rock, South Pars, Subsidence.

INTRODUCTION

Withdrawal of subsurface fluids such as groundwater, oil, and gas is a major cause for ground subsidence in the recent decades. Although, subsidence caused by oil and gas withdrawal is very limited compared to groundwater extraction, due to the economical importance of oil and gas fields and the great effects of subsidence on exploitation operations of fields, evaluation of this phenomenon is highly recommended. Reservoir compaction will reduce porosity and permeability of reservoir rock which will decrease the flow of hydrocarbon fluid towards production wells and can also cause

casing collapse. Subsidence may cause operational problems such as overwhelm of platform in offshore production. On land, subsidence may significantly increase the risk of damage to buildings and infrastructure (Fokker et al., 2007). Therefore, prediction of surface subsidence in the South Pars gas field that is a shared field between Iran and Qatar is very important. The Ekofisk field is one of the well-known examples of the subsided hydrocarbon fields. In 1984, the seabed under the operational platform had subsided over 3 m, and the remediation operation cost approached one billion dollars (Sulak, 1991). At the end of 2000, the subsidence of the

* Corresponding author E-mail: mh.taherynia@gmail.com

Ekofisk reached to 6.7 m and was continuously subsiding at a fairly constant rate (Hermansen et al., 2000), at about 0.4 m/year. The other well-known example of subsided oil field is the Wilmington oil field in California, which has experienced 9 meters of subsidence (Mayuga and Allen, 1969). The annual rate of surface subsidence in the Wilmington field was up to 70 cm (Gurevich and Chilingarian, 1995). Oil fields in the east coast of Maracaibo Lake in Venezuela experience significant subsidence between 1926 and 2004. The subsidence in these fields exceeded 5 m in 1988, and resulted in severe flooding of more than 450 km² of land near the coast of Lake Maracaibo (Atefi Monfared 2009). Reservoir compaction and field surface subsidence also

can cause formation and expansion of fractures in the caprock. This may impair the caprock's reliability and provide some paths for the leakage of gas (Gurevich and Chilingarian, 1995).

The South Pars/North Dome gas field in the Persian Gulf is the largest offshore gas field in the world and is located at 105 Km southwest of the Asaluyeh port of Iran at E52° to 52.5° and N26.5 to 27°. According to the International Energy Agency (IEA), the field holds an estimated 51 trillion cubic meters of in-situ natural gas and a 7.9 billion cubic meters of natural gas condensates. The area of this field is 9700 Km², in which South Pars, belonging to Iran, is 3700 Km² and the rest, North Dome, belongs to Qatar (Figure 1).

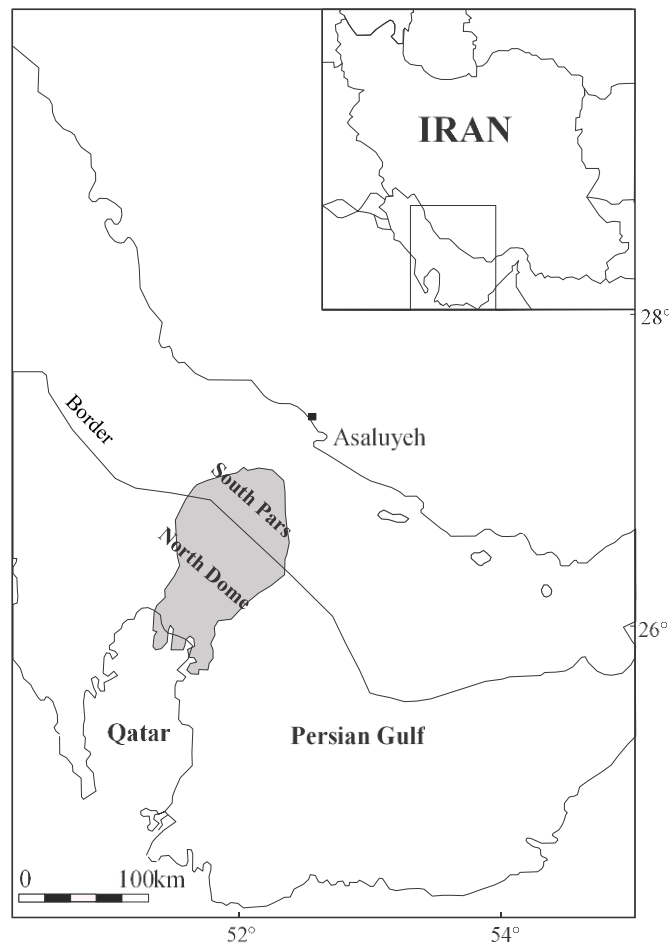


Fig. 1. Geographical location of the South Pars/North Dome gas field.

The South Pars/North Dome gas field is a part of the huge NNE–SSW trend of Qatar Arch structural feature. The Kangan Formation and the Upper Dalan Member with a Permian–Triassic age collectively formed the South Pars reservoir (Figure 2). The Kangan and Dalan Formations together are equivalent to the Khuff Formation in the Arabian nomenclature. The Kangan and Dalan Formations are separated by an impermeable layer. Each formation is divided into two different reservoir layers that are separated by impermeable barriers. Therefore, as it is shown in Figure 2, the

field consists of four independent reservoir layers: K1, K2, K3, and K4 (Rahimpour-Bonab, 2007). The rocks of the reservoir are mainly carbonates e.g. dolomite, limestone, recrystallized limestone, and replacive dolomite. Vuggy porosity is the dominant porosity type in this reservoir (Pars Oil & Gas Company, 2003-4). The carbonate rocks of the reservoir, based on Dunham (1962) classification, can be classified as mudstone, grainstone and packstone, and based on their allochem size can be classified as fine grained and coarse grained.

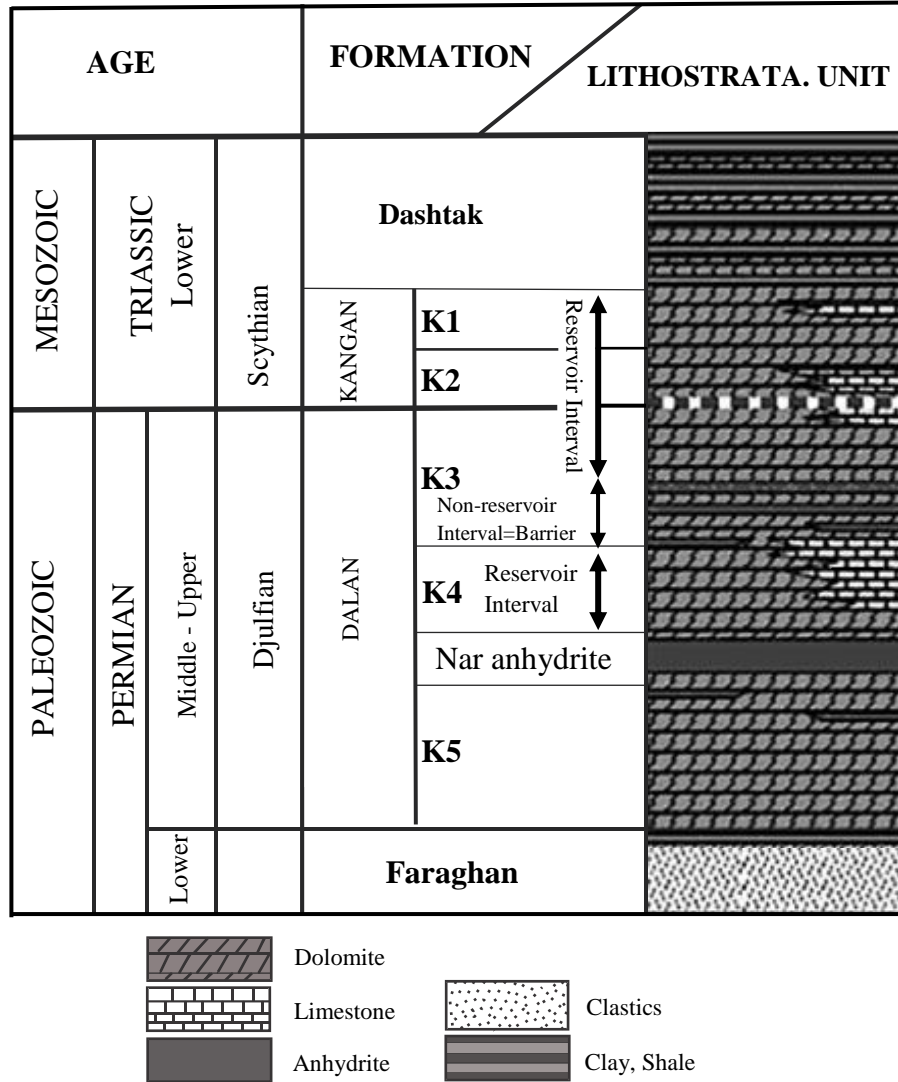


Fig. 2. Stratigraphic chart of the South Pars gas field and its main reservoir members (Rahimpour-Bonab, 2007).

MATERIALS AND METHODS

As mentioned above, the first step for determination of surface subsidence in oil and gas field is calculation of the reservoir compaction. Vertical deformation of reservoir rock by using Hooke's law in terms of changes of major stress to original state of stress (before extraction) can be expressed as:

$$\varepsilon_v = \frac{\Delta h}{h} = \frac{1}{E_i} [\Delta\sigma'_v - \nu_i(\Delta\sigma'_h + \Delta\sigma'_H)] \quad (1)$$

where Δh is the change of reservoir thickness, in other words, the amount of reservoir compaction, h is initial reservoir thickness, E_i is Young's modulus of frame reservoir rock, ν_i is the Poisson's ratio of reservoir rock and $\Delta\sigma'_v$, $\Delta\sigma'_H$ and $\Delta\sigma'_h$ are the changes in three effective major vertical and horizontal stresses, respectively. For simplification, Geertsma (1973) assumed that the stress arching does not occur and therefore the entire overburden load is imposed over reservoir rock during extraction and the vertical stress stays constant. Since the overburden load is constant, any change in the effective vertical stress will be due to a reduction of the reservoir pressure and can be calculated as follows:

$$\Delta\sigma'_v = \Delta\sigma_v - \alpha\Delta P = -\alpha\Delta P \quad (2)$$

The change in effective horizontal stress (assuming they are equal) due to changes of the effective vertical stress by using horizontal stress path coefficient (K) can be expressed as:

$$\Delta\sigma'_H = \Delta\sigma'_h = K\Delta\sigma'_v \quad (3)$$

Hence, by inserting changes in the three major stresses into Eq. (1), the following equation can be obtained as:

$$\varepsilon_v = -\frac{1}{E_i}(1-2\nu_i K)\alpha\Delta P = Cm \times \alpha\Delta P \quad (4)$$

where Cm is the uniaxial compressive coefficient. The compressibility of the reservoir has a reverse relation with K . The coefficient of horizontal stress path can be calculated by either equations presented by Terzaghi and Richart (1952) (Eq. (5)) for sound reservoir rock or Addis (1997) (Eq. (6)) for fractured reservoir rock.

$$K = \frac{\nu_i}{1-\nu_i} \quad (5)$$

$$K = \frac{1-\sin\varphi}{1+\sin\varphi} \quad (6)$$

where φ is the angle of internal friction of reservoir rock.

The South Pars reservoir cannot be considered as either jointed or sound reservoir, because the present joints are usually classified as micro fractures and the dominant porosity of the reservoir is a Vuggy type of porosity. Thus, it is difficult to define the reservoir's stress path. In order to determine the stress path, the calculated results from Eqs. (5) and (6) were compared with the results of breakout analysis performed in the field. The comparison indicates that the South Pars reservoir will probably experience the stress path coefficient that was calculated by equation described by Addis (1997) during field extraction.

Six main reservoir rock types with different elastic properties were identified in the South Pars reservoir. Some mechanical properties of these rock layers such as the uniaxial compaction coefficient (Cm) and

predicted change of thickness of each layer at the end of the extraction period are presented in Table 1. The initial reservoir pressure is about 36.5 MPa that will reduce to 6.2 MPa at the end of the extraction period.

Table 1. Characteristics of reservoir rock mass and the thickness change predicted at the end of extraction.

Reservoir Layers	Biot Coefficient (α)	K	Cm (MPa ⁻¹)	Δh (m)
L1	0.89	0.11	0.000124	0.05
L2	0.83	0.22	0.000023	0.08
L3	0.82	0.23	0.000035	0.05
L4	0.85	0.42	0.00011	0.17
L5	0.93	0.32	0.000076	0.10
L6	0.87	0.4	0.000025	0.02

According to Table 1 the total compaction (Δh) of the South Pars reservoir will reach to about 0.48 m at the end of the extraction period.

According to Geertsma (1973) if the predicted reservoir compaction is lower than 10 cm, there is little need to follow the matter further. On the other hand, if larger values are obtained, field surface subsidence can be problematic. Hence, with respect to the value of the South Pars reservoir compaction, there is a probability of problematic surface subsidence in this field that needs further studies to accurately assess the resulted surface subsidence.

The next step indetermination of the field surface subsidence is modeling the effect of the reservoir compaction on the surface. Sroka and Hejmanowski (2006) proposed that the compacting reservoir can be divided into cubic elements (Figure 3) and the subsidence caused by compaction of each cubic element can be obtained as:

$$\Delta S = K_z \times \Delta V \tag{7}$$

where ΔS is subsidence, K_z is the influence function, and ΔV is volume reduction of the reservoir element that is equal to the element surface area multiplied by the element compaction (Δh).

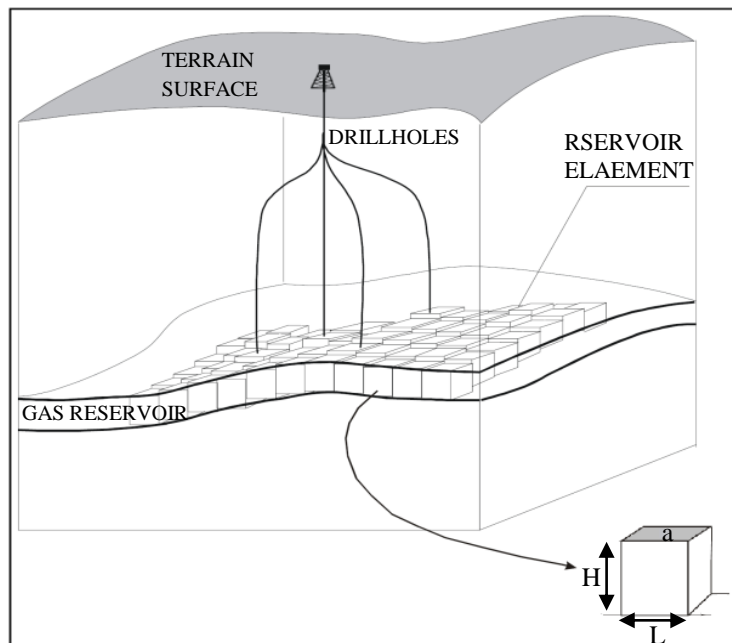


Fig. 3. Dividing of reservoir into the cubic shape elements (Sroka and Hejmanowski, 2006).

For determination of the whole reservoir compaction effect on the field surface Eq. (7) can be used as:

$$dS = \Delta h \int_A K_z da \quad (8)$$

where A is the total surface area of the reservoir.

Bals (1932) presented the influence function for the first time for estimation of surface deformation. Since then, many researchers have conducted studies on this subject. One of the most common and applicable influence functions for prediction of subsidence in oil and gas field is the Geertsma (1973) proposed function, which was presented as below:

$$K_z = \frac{1-\nu}{\pi} \cdot \frac{D}{(r^2 + D^2)^{3/2}} \quad (9)$$

where D is reservoir depth and r is the horizontal distance of the calculating point from the compacted reservoir element.

The above equation is applicable for a reservoir with a well-defined geometry. Reddish et al. (1994) presented a method for predicting subsidence above a reservoir with complex geometry. They used a network of several series of concentric circle bands with

equal widths, equally divided by radius lines (Figure 4).

The influence of each one of the circular band on the central point of the network can be calculated by substituting Geertsma's influence function with Eq. (8) and integrating over the band surface as follows:

$$K_z(i) = 2(1-\nu) \left(\frac{1}{\sqrt{\left(\frac{r_{i-1}}{D}\right)^2 + 1}} - \frac{1}{\sqrt{\left(\frac{r_i}{D}\right)^2 + 1}} \right) \quad (10)$$

The divided zones in each ring, with respect to their equal distances from the center of network, have equal influence factors, which can be calculated as:

$$K_{z(z_i)} = \frac{K_z(i)}{N_{z_i}} \quad (11)$$

where N_{z_i} is the number of zones in the ring i .

Ultimately, the subsidence of the field caused by the whole reservoir compaction can be calculated by the following equation:

$$S = \Delta h \sum K_{z(z_i)} \times N_{(i)} \quad (12)$$

where $N(i)$ shows the number of covered zones of ring i by the reservoir.

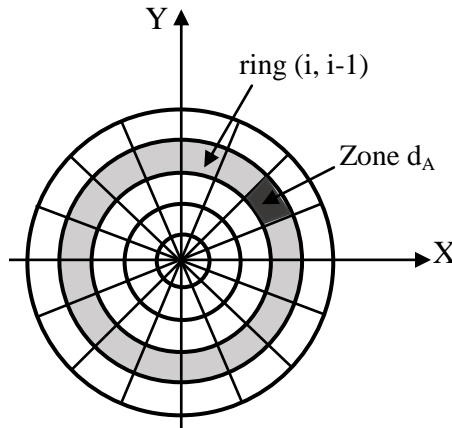


Fig. 4. The network with circular zones that equally divided by radial lines (Raddish et al., 1994).

RESULTS AND DISCUSSION

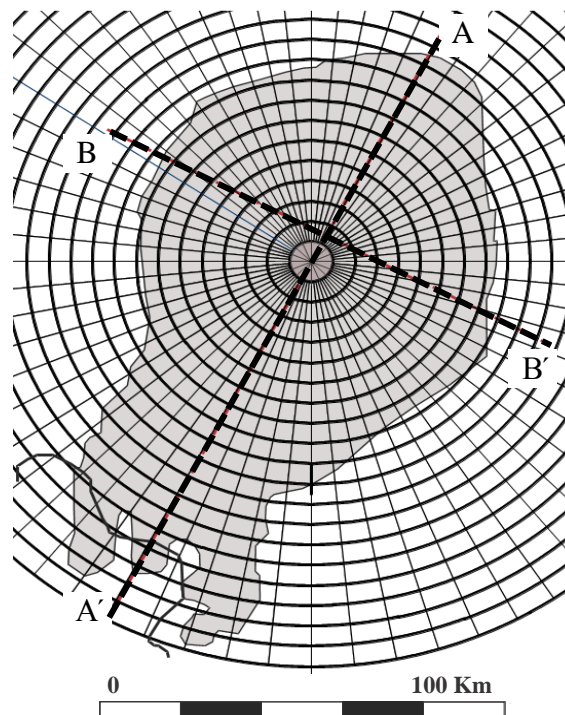
In this study, we used a network with 20 rings that all of them, except the first ring, were divided into 64 zones. The first ring, due to the high density of the radial lines, was divided into 16 zones. Figure 5 shows that the South Pars reservoir is compatible with the network and the influence coefficient of each ring of the network.

To determine the subsidence profile along two lines of A_A' and B_B', the center of the network is put on different points on the lines and the number of matched zones of each ring with the reservoir is counted.

In addition to the presented analytical method, the semi-analytical method presented by Fokker and Orlic (2006), implemented in the AEs subs software was used for subsidence modeling. The method used combinations of analytical solutions for solving the visco-elastic equations in such a way that the boundary conditions at layer interfaces and the ground surface are

approximated. The solution obtained by this method yields an influence function in conjunction with the reservoir and subsurface layers properties. This influence function is used in a similar way to the Sroka and Hejmanowski (2006) approach for determination of the subsidence bowl that was caused by the whole reservoir compaction. The main advantage of the semi-analytical method is its higher accuracy and flexibility for complex conditions of reservoir and overburden. As mentioned above, the application of analytical methods is limited to homogeneous reservoir and adjacent environment, but in semi-analytical methods, there is the possibility for modeling of the environment with several layers that have different characteristics. This method is much simpler and needs less time than numerical methods.

The subsidence bowls predicted by the analytical and the semi-analytical methods are shown in Figures 6 and 7.



Ring	KZ(i)
1	0.526
2	0.2141
3	0.0833
4	0.0432
5	0.0263
6	0.0177
7	0.0127
8	0.0095
9	0.0074
10	0.006
11	0.0049
12	0.0041
13	0.0034
14	0.003
15	0.0026
16	0.0022
17	0.002
18	0.0018
19	0.0016
20	0.0014

Fig. 5. Plan of the South Pars reservoir matched with the influence network.

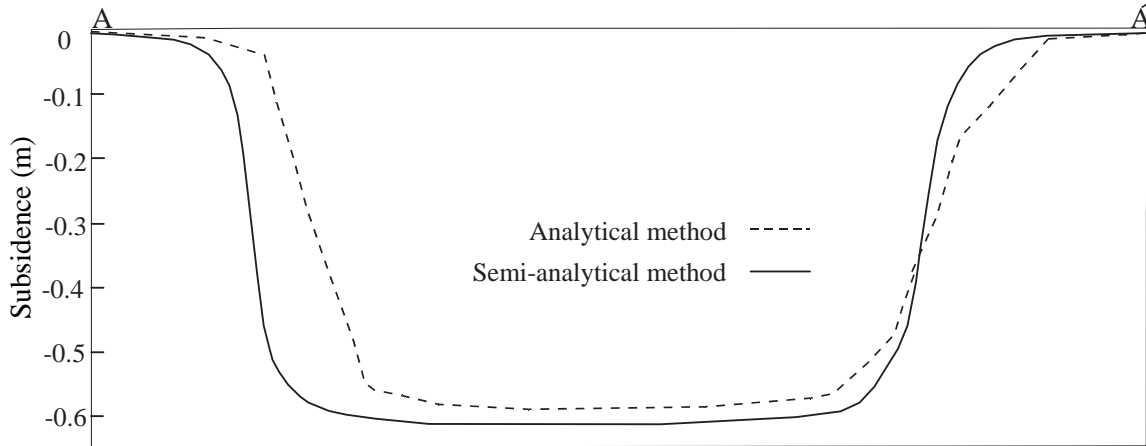


Fig. 6. Cross section of the subsidence bowl along A-A' line calculated by the analytical and the semi-analytical methods.

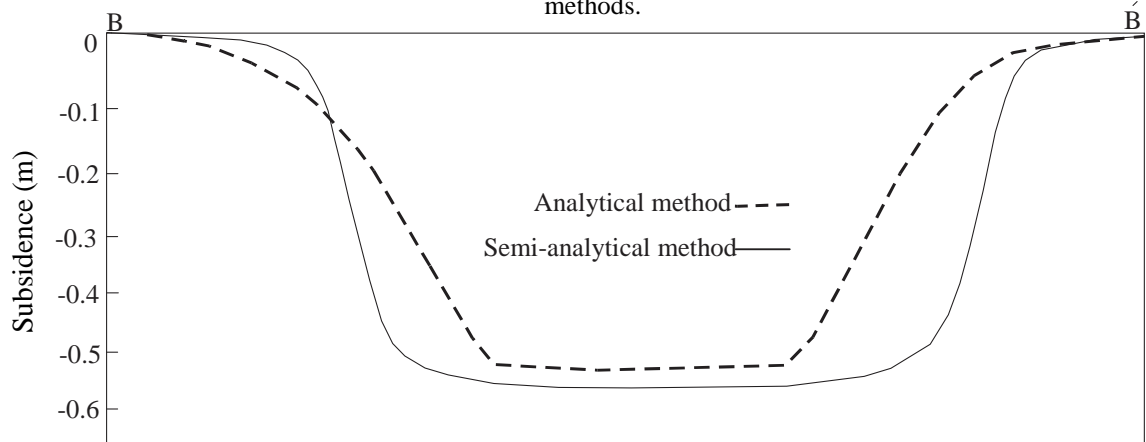


Fig. 7. Cross section of the subsidence bowl along B-B' line calculated by the analytical and the semi-analytical methods.

As shown in the Figures 6 and 7, the maximum subsidence predicted using both methods are approximately equal, but there are significant differences between modeled subsidence bowls at the reservoir edges. One reason for the observed differences in the subsidence bowl shapes is due to the inability of the analytical method for modeling of multi layers subsurface and treating the layered subsurface as a homogeneous media. Also in the Geertsma's influence function (Eq. (9)) Poisson's ratio for determining the effect of reservoir compaction on the field surface is only used. But in the semi-analytical methods, in addition to Poisson's ratio, Young's modulus and other (visco-) elastic properties

of subsurface layers are used. Modeling of surface subsidence using the AEs subs software indicated that the Young's modulus of the overburden rock layers have great effects on the predicted subsidence bowl shape. According to these modeling results, increase of Young's modulus will decrease the volume of subsidence bowl (depth and width).

The plan of the subsidence bowl calculated by the AEs subs software is presented in Figure 8.

The important point about the results of modeling is that the amount of predicted subsidence is larger than the reservoir compaction. According to Geertsma (1973) this matter can be caused by downward

displacement of the reservoir bottom. The modeling of displacement around compacting reservoir that was carried out by Fjær et al. (2008) indicated that, the upper part of the disk shape reservoir with radius equal to the depth is displaced downward. The bottom of the reservoir is displaced upward which results in lowering of field surface subsidence compare to compaction

of the reservoir. On the other hand, both upper and bottom parts of wide reservoir (with a radius three times higher than its depth) are displaced downward in which the resulting subsidence is more than the compaction of the reservoir. By using the AEs subs software, vertical displacements of bottom part of the reservoir is modeled and presented in Figure 9.

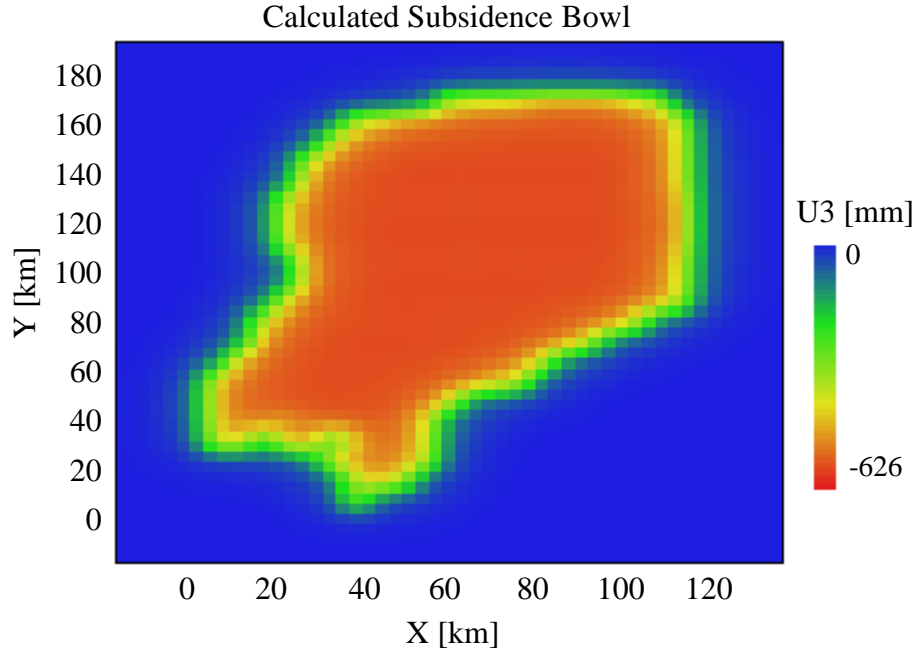


Fig. 8. Plan of subsidence bowl modeled by the AEs subs software.

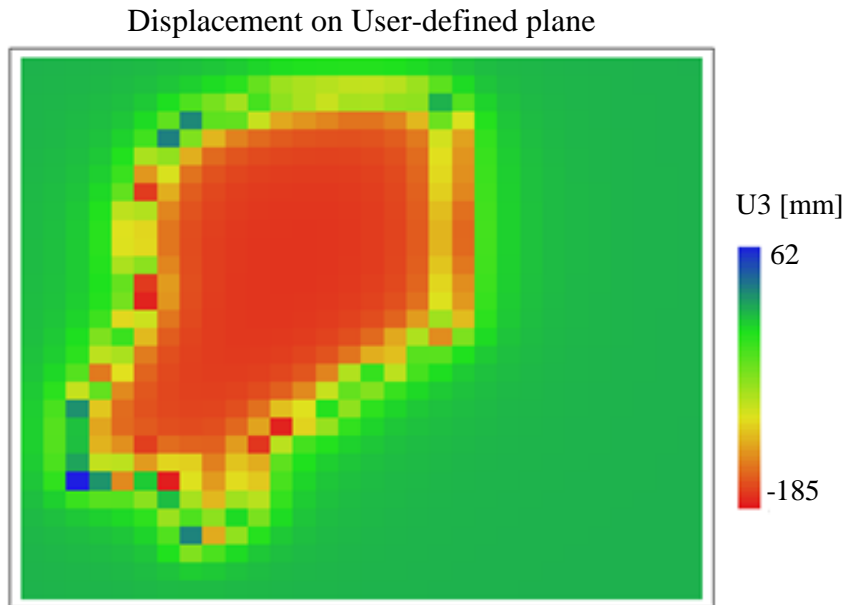


Fig. 9. Vertical displacement of the reservoir bottom predicted by the AEs subs software.

CONCLUSIONS

The amount of the reservoir compaction at the end of exploitation of the South Pars gas field was calculated to be about 0.48 m. Both the analytical and the semi-analytical methods used for subsidence modeling of the South Pars/North Dome field showed almost similar results. According to both modeling methods, the maximum surface subsidence of field is predicted to be about 0.6 m. The results indicated that, due to downward displacement of the reservoir bottom, the amount of predicted subsidence is higher than the calculated reservoir compaction. According to modeling by the AEsubs software the bottom of the reservoir has about 0.18 m downward displacement. The ratio of the subsidence to the reservoir compaction of South Pars/North Dome field is about 1.3. With respect to the reservoir radius it is much larger than the reservoir depth, this phenomenon is predictable. According to Fjær et al. (2008) in very wide reservoirs, the ratio of the subsidence to the reservoir compaction approaches 1.5.

ACKNOWLEDGEMENT

The authors would acknowledge Dr. Peter Fokker for his great advices and recommendations, thank the TNO Company for supplying AEsubs software. The authors wish to thank Dr. Mazda Kompani Zare and Mr. Abbasali Porteghali for their useful advices. The authors appreciate the support of National Iranian Oil Company for data preparation and permission to publish this paper.

REFERENCES

Addis, M. (1997). "The stress-depletion response of reservoirs", *SPE Annual Technical Conference and Exhibition*, Society of Petroleum Engineers San Antonio, Texas, pp. 55-65.

- Bals, R. (1932). "Beitrag zur frage der vorausberechnung bergbaulicher senkungen. mitt. aus dem markscheidewesen", *Mitt. Markscheidew.*, 42-43, 98-111.
- Atefi Monfared, K. (2009). "Monitoring oil reservoir deformations by measuring ground surface movements", M.Sc. Thesis, Ontario, Canada, University of Waterloo, *Master of Applied Science*, p. 256.
- Dunham, R.J. (1962). "Classification of carbonate rocks according to depositional texture", In: Hamm, W.E. (Ed.), *Classification of Carbonate Rocks-A Symposium*. American Association of Petroleum Geologists, Memoir No. 1. Tulsa, Oklahoma, pp. 108-121.
- Fjær, E., Holt, R., Horsrud, P., Raaen, A. and Risnes, R. (2008). *Petroleum related rock mechanics*, Elsevier Science Publishers B.V., Amsterdam.
- Fokker, P. and Orlic, B. (2006). "Semi-analytic modelling of subsidence", *Mathematical Geology*, 38(5), 565-589.
- Fokker, P.A., Muntendam-Bos, A.G. and Kroon, I.C. (2007). "Inverse modelling of surface subsidence to better understand the earth's subsurface", *First Break*, 25(8), 101-105.
- Geertsma, J. (1973). "Land subsidence above compacting oil and gas reservoirs", *Journal of Petroleum Technology*, 25(6), 734-744.
- Gurevich, A.E. and Chilingarian, G.V. (1995). "Chapter 4: Possible impact of subsidence on gas leakage to the surface from subsurface oil and gas reservoirs", *Developments in Petroleum Science*, Elsevier, Amsterdam, pp. 193-213.
- Hermansen, H., Landa, G., Sylte, J. and Thomas, L. (2000). "Experiences after 10 years of waterflooding the Ekofisk Field, Norway", *Journal of Petroleum Science and Engineering*, 26(1), 11-18.
- Mayuga, M.N. and Allen, D.R. (1969). "Subsidence in the Wilmington oil field, Long Beach, Californai, USA", *Proceedings of the Tokyo Symposium: International Association of Scientific Hydrology*, pp. 66-79.
- Rahimpour-Bonab, H. (2007). "A procedure for appraisal of a hydrocarbon reservoir continuity and quantification of its heterogeneity", *Journal of Petroleum Science and Engineering*, 58(1), 1-12.
- Reddish, D., Yao, X. and Waller, M. (1994). "Computerised prediction of subsidence over oil and gas fields", *Rock Mechanics in Petroleum Engineering (Eurock'94)*, Society of Petroleum Engineers Delft, Netherlands, pp. 621-630.
- Sroka, A. and Hejmanowski, R. (2006). "Subsidence prediction caused by the oil and gas

development”, 3rd IAG Symposium on Geodesy for Geotechnical and Structural Engineering and 12th FIG Symposium on Deformation Measurements, Baden, Austria, p. 8.

Sulak, R.M. (1991). “Ekofisk field: the first twenty years”, *Journal of Petroleum Technology*, 43(10), 1265-1271.

Terzaghi, K., Richart, F.E. (1952). “Stresses in rock about cavities”, *Geotechnique*, 3(2), 57-90.